Natural convection in a nanofluid-filled enclosure with partially heated on side wall

†Vai Kuong Sin, *Pengxiang Sui

[1]Department of Electromechanical Engineering, University of Macau, Macau SAR, China.
[2]Department of Electromechanical Engineering, University of Macau, Macau SAR, China

*Presenting author: YB77437@um.edu.mo
†Corresponding author: vksin@um.edu.mo

Abstract

The buoyant flow and heat transfer in the enclosure filled with nanofluid is investigated numerically in this paper. The heated source is located on the left side-wall with constant heat flux, the right side-wall kept constant temperature and the top and bottom walls of the enclosure are insulated. The governing equations are solved by using the finite element method. The influences of the variable Rayleigh number, volume fractions, length of the heated source and different types of nanofluids are studied. Results are performed as the streamline and isotherm plots as well as the variation of the local and mean Nusselt number. It is observed from the result that the increase of Rayleigh number enhances buoyant flow and causes increasing mean Nusselt number on the heated source. In addition, the increasing heated source length investigated significantly effect on maximum temperature along the heated source. It is shown that the increase of volume fraction improves the thermal conductivity of the nanofluid. Finally, the nanofluid has a better cooling performance by compared with pure water.

Keywords: Natural convection, Nanofluid, Partially heated source, Rayleigh number

Introduction

Natural convection in the enclosure has wide applications in industry and engineering, such as electronic cooling system, biological sciences, material science and heat exchangers. Enhancement of heat transfer in natural convection is a necessary topic from saving energy and improving efficiency.

Majority of the present studies on thermal properties of the nanofluid presence the nanoparticles in the fluids can increase the effective thermal conductivity and enhance the heat transfer characteristics. Nanofluid is a dilute suspension of solid nanoparticles with a size typically of 1-100 nm dispersed in the liquid. The small solid nanoparticles at low volume fraction in liquid changes in physical properties, such as density, dynamic viscosity and specific heat, which can enhance the thermal conductivity and increase in critical heat flux in boiling heat transfer over the base-fluid value [1]-[4]. The nanofluids are a new class of heat transfer fluids by consisting of different nanoparticles. Masuda et al. [5] investigated different nanofluids CuO-water , Al_2O_3-water , SiO_2-water and TiO_2-water enhanced the thermal conductivity of nanofluids at a small volume fraction. This thermal property enhancement phenomenon was also reported by Eastman et al. [6].

Many studies of natural convection in enclosure are considered under the assumption of heated by constant temperature or heated by constant heat flux. Oztop and Abu -Nada [7] employed the finite volume method to investigate heat transfer and fluid flow due to the buoyancy forces in a partially heated rectangular enclosure for different types of nanofluids. The results indicated heat transfer enhancement by using nanofluids and was more pronounced at low aspect ratios than at high aspect ratios and the mean Nusselt number increased as increasing the volume fraction of nanoparticles for the entire range of Rayleigh number. Another study of natural convection in a square cavity with partially active side-walls filled with Cu-water nanofluid is investigated by Sheikhzadeh et al. [8]. The active heated sources are on both vertical side-walls of the cavity at the constant temperature. The effects of locations of the active heated sources, the Rayleigh number and the nanoparticle's volume fraction were studied and the results showed that the average Nusselt number increases with increasing both the Rayleigh number and the volume fraction of the nanoparticles.

Cheikh et al. [9] studied natural convection in air-filled square enclosure heated with the constant heat flux from below and cooled from above for different thermal boundary conditions. The simulations are performed for two different lengths of the heated sources and several Rayleigh number. The results are presented by streamline and isotherm plots and the maximum temperature along the heated source surface. Aminossadati and Ghasemi [10] also investigated a numerical study of natural convection cooling of the constant heat flux source on the bottom wall of the enclosure. Various Rayleigh number, location, and geometry of the heated source, different types of nanofluids and volume fractions are studied and the results showed nanofluids can enhance cooling performance, especially at low Rayleigh number, and the maximum temperature at heated source is based on the length and location of heated source, and type of nanofluids.

Despite several numerical studies and experimental which investigated natural convection in enclosure with different thermal boundary conditions. There is no study has been reported in the literature which investigated the enclosure heated by constant heat flux on one side-wall and cooling at constant temperature on the other side-wall. This problem may be encountered in a number of electronic cooling systems. In this paper, the aim of present study is to study fluid flow and heat transfer in the enclosure at a constant heat flux on the left side-wall and cooled from the right side-wall by constant temperature. The results are showed by streamline and isotherm plots with different Rayleigh number and volume fractions, the maximum temperature along heated source and mean Nusselt number also would be analyzed and discussed in this paper.

Problem Description

Figure 1 shows the physical model of partially heated source enclosure with the length L. The heated source with constant heat flux q'' is located on the left side-wall of enclosure and the length of heated source is e. The distance of heated source center from the bottom wall is d. The right side-wall is kept at the constant low temperature T_c and the top and bottom walls are thermally insulated. The enclosure is filled with nanofluid, which is assumed incompressible and flow as laminar within the enclosure. The thermo-physical properties of base fluid and various nanofluids are given in Table 1 [11]. Also, the nanofluid's thermo-physical properties are assumed constant except for its density variation which is depended on the Boussinesq approximation.

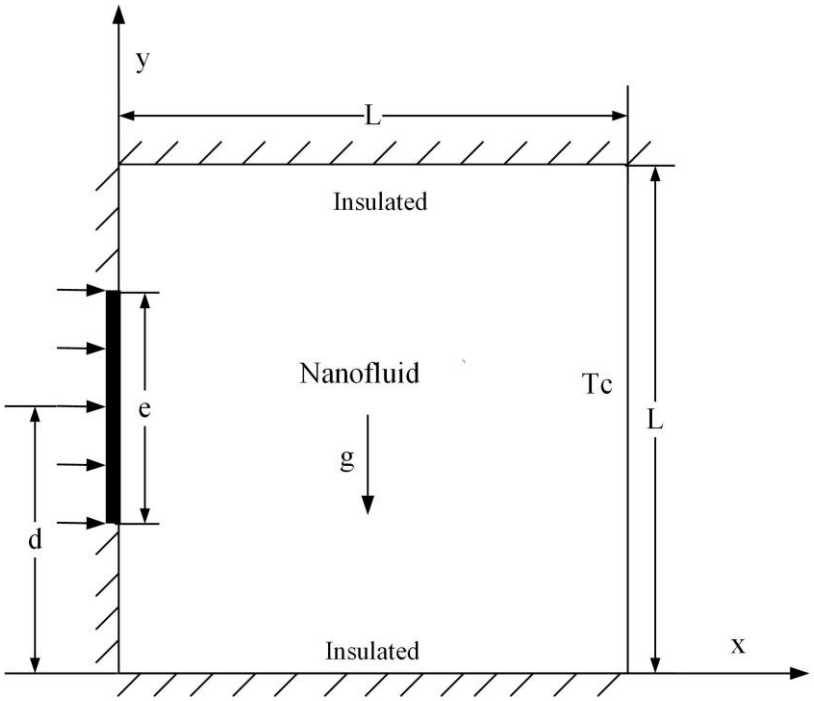

Figure 1. Geometry and coordinate system of the enclosure

Table 1. Thermo-physical properties of the base fluid and various nanoparticles

	Density $\rho\ (kg/m^3)$	Specific Heat $C_p\ (J/kgK)$	Thermal Conductivity $k\ (W/mK)$	Thermal Expansion Coefficient $\beta \times 10^{-5}\ (1/K)$
Pure Water	997.1	4179	0.613	21
Copper	8933	385	401	1.67
Alumina	3970	765	40	0.85
Titanium Oxide	4250	686.2	8.9538	0.9

Governing Equation

The steady-state natural convection in terms of continuity, momentum and energy equations for buoyancy-driven flow within the enclosure are given by:

Continuity equation

$$\frac{\partial u}{\partial x} + \frac{\partial v}{\partial y} = 0 \qquad (1)$$

where *u* and *v* are the velocity components in x and y direction

Momentum equations

$$\rho_{nf}\left(u\frac{\partial u}{\partial x}+v\frac{\partial u}{\partial y}\right)=-\frac{\partial p}{\partial x}+\mu_{nf}\left(\frac{\partial^2 u}{\partial x^2}+\frac{\partial^2 u}{\partial y^2}\right) \quad (2)$$

$$\rho_{nf}\left(u\frac{\partial v}{\partial x}+v\frac{\partial v}{\partial y}\right)=-\frac{\partial p}{\partial x}+\mu_{nf}\left(\frac{\partial^2 v}{\partial x^2}+\frac{\partial^2 v}{\partial y^2}\right)+g(\rho\beta)_{nf}(T-T_C) \quad (3)$$

where ρ_{nf} is the density of nanofluid, μ_{nf} is the dynamic viscosity of nanofluid, p is the pressure, β is the thermal expansion coefficient.

Energy equation

$$u\frac{\partial T}{\partial x}+v\frac{\partial T}{\partial y}=\alpha_{nf}\left(\frac{\partial^2 T}{\partial x^2}+\frac{\partial^2 T}{\partial y^2}\right) \quad (4)$$

where T is the temperature and α is the fluid thermal diffusivity.

The effective density of nanofluid is given as

$$\rho_{nf}=(1-\emptyset)\rho_f+\emptyset\rho_s \quad (5)$$

where ρ_f is the density of fluid, ρ_s is the density of solid nanoparticle and $\emptyset$ is the volume fraction.

The effective heat capacitance of the nanofluid can be determined by

$$(\rho C_p)_{nf}=(1-\emptyset)(\rho C_p)_f+\emptyset(\rho C_p)_s \quad (6)$$

where C_p is the specific heat.

The effective thermal expansion coefficient of the nanofluid given as

$$(\rho\beta)_{nf}=(1-\emptyset)(\rho\beta)_f+\emptyset(\rho\beta)_s \quad (7)$$

The dynamic viscosity of the nanofluid given by the Brinkman [12] as

$$\mu_{nf}=\frac{\mu_f}{(1-\emptyset)^{2.5}} \quad (8)$$

The effective thermal conductivity of the nanofluid can be approximated by the Maxwell-Garnetts [13] as

$$k_{nf} = k_f \left[\frac{k_s + 2k_f - 2\emptyset(k_f - k_s)}{k_s + 2k_f + \emptyset(k_f - k_s)} \right] \quad (9)$$

where k_f and k_s are the thermal conductivities of base fluid and nanoparticle.

The thermal diffusivity of the nanofluid is expressed by

$$\alpha_{nf} = \frac{k_{nf}}{(\rho C_p)_{nf}} \quad (10)$$

Equations (1) to (4) can be converted to dimensionless forms, and the dimensionless variables are (dimensionless coordinate X and Y, dimensionless velocity U and V, dimensionless pressure P, reference temperature different ΔT and dimensionless temperature θ)

$$X = \frac{x}{L}, \quad Y = \frac{y}{L}, \quad U = \frac{uL}{\alpha_f}, \quad V = \frac{vL}{\alpha_f}, \quad P = \frac{pL^2}{\rho_{nf}{\alpha_f}^2}, \quad \Delta T = \frac{q''L}{k_f}, \quad \theta = \frac{(T-T_c)k_f}{q''L} \quad (11)$$

The dimensionless governing equations of continuity, momentum and energy equations are given as follows

Dimensionless continuity equation

$$\frac{\partial U}{\partial X} + \frac{\partial V}{\partial Y} = 0 \quad (12)$$

Dimensionless momentum equations

$$U\frac{\partial U}{\partial X} + V\frac{\partial U}{\partial Y} = -\frac{\partial P}{\partial X} + \frac{\mu_{nf}}{\rho_{nf}\alpha_f}\left(\frac{\partial^2 U}{\partial X^2} + \frac{\partial^2 U}{\partial Y^2}\right) \quad (13)$$

$$U\frac{\partial V}{\partial X} + V\frac{\partial V}{\partial Y} = -\frac{\partial P}{\partial X} + \frac{\mu_{nf}}{\rho_{nf}\alpha_f}\left(\frac{\partial^2 V}{\partial X^2} + \frac{\partial^2 V}{\partial Y^2}\right) + \frac{(\rho\beta)_{nf}}{\rho_{nf}\beta_f} RaPr\theta \quad (14)$$

Dimensionless energy equation

$$U\frac{\partial \theta}{\partial X} + V\frac{\partial \theta}{\partial Y} = -\frac{\alpha_{nf}}{\alpha_f}\left(\frac{\partial^2 \theta}{\partial X^2} + \frac{\partial^2 \theta}{\partial Y^2}\right) \quad (15)$$

In above equations, the Rayleigh number and Prandtl number are defined by

$$Ra = \frac{gq''L^4\beta_f}{{v_f}^2 k_f} \times Pr, \qquad Pr = \frac{v_f}{\alpha_f} \quad (16)$$

where v_f is the kinematic viscosity of fluid.

The boundary conditions for equations (12) – (15) in dimensionless form are as follows

$$\begin{aligned}
&\mathrm{U}=\mathrm{V}=0, \quad \frac{\partial\theta}{\partial X}=0 && \text{for } \mathrm{X}=0 \text{ and } 0\le \mathrm{Y}\le \mathrm{D}-0.5\mathrm{E} \text{ and } \mathrm{D}+0.5\mathrm{E}\le \mathrm{Y}\le 1\\
&\mathrm{U}=\mathrm{V}=0, \quad \frac{\partial\theta}{\partial X}=-\frac{k_f}{k_{nf}} && \text{for } \mathrm{X}=0 \text{ and } \mathrm{D}-0.5\mathrm{E}\le \mathrm{Y}\le \mathrm{D}+0.5\mathrm{E}\\
&\mathrm{U}=\mathrm{V}=0, \quad \frac{\partial\theta}{\partial Y}=0 && \text{for } \mathrm{Y}=1 \text{ and } 0\le \mathrm{X}\le 1\\
&\mathrm{U}=\mathrm{V}=0, \quad \theta=0 && \text{for } \mathrm{X}=1 \text{ and } 0\le \mathrm{Y}\le 1\\
&\mathrm{U}=\mathrm{V}=0, \quad \frac{\partial\theta}{\partial Y}=0 && \text{for } \mathrm{Y}=0 \text{ and } 0\le \mathrm{X}\le 1
\end{aligned} \qquad (17)$$

The local Nusselt number of heated source is calculated from the following equations

$$Nu_{local}=\frac{hL}{k_f} \qquad (28)$$

$$h=\frac{q''}{T_{local}-T_c} \qquad (19)$$

where T_{local} is the local temperature along the heated source.

The local Nusselt number by using dimensionless variables are given by

$$Nu_{local}=\frac{1}{\theta_s(X)} \qquad (20)$$

The mean Nusselt number is determined by integrating Nu_{local} along the heated source on the left side-wall as

$$Nu_m=\frac{1}{E}\frac{k_{nf}}{k_f}\int_{Y_1}^{Y_2}\frac{1}{\theta_s(X)}dx \qquad (21)$$

where E is the dimensionless length of heated source (e/L), D is the dimensionless distant of heated source center from the bottom wall (d/L), and $Y_1=D-0.5E$ and $Y_2=D+0.5E$.

Validation

COMSOL Multiphysics software is used to solve the governing equation, which employs Boussinesq term and dimensionless parameters for buoyant flow driven with the laminar flow and the heat transfer coupled interfaces. The present simulation results are also validated against the numerical results by Cheikh et al. [9] and S.M. Aminossadati et al. [10]. Figure 2 presents geometry of the air-filled square enclosure in study of Cheikh. Both two vertical side-walls cooled at constant temperature T_c and the top and the bottom wall are insulated. The enclosure heated by the heated source from below. Table 2 gives the value of the mean Nusselt number along the heated source on the bottom wall of the enclosure, and the

maximum temperature within enclosure for various Rayleigh number and two different lengths of the heated source.

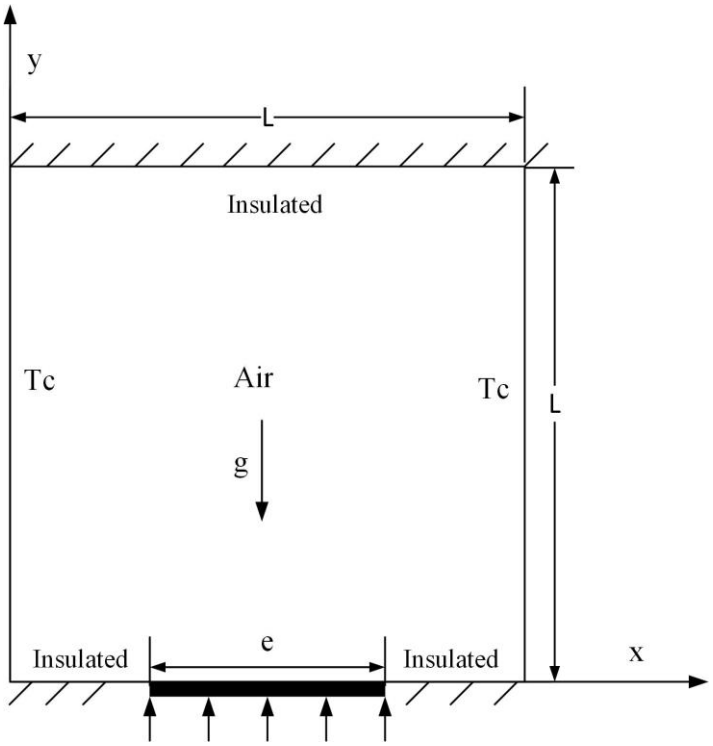

Figure 2. Geometry and coordinate system of the enclosure in study of Cheikh [9]

Table 2. Comparisons of the present simulation results with the other studies

			Rayleigh Number				
			10^3	10^4	10^5	10^6	10^7
E=0.2	Nu_m	Present work	5.9487	5.9808	7.6353	12.1218	19.9414
		Cheikh et al	5.9152	5.9467	7.5805	12.0390	19.9801
		Aminossadati et al	5.9228	5.9539	7.5910	12.0624	20.0195
	T_{max}	Present work	0.1818	0.1815	0.1484	0.1042	0.0734
		Cheikh et al	0.1819	0.1815	0.1484	0.1040	0.0730
		Aminossadati et al	0.1819	0.1815	0.1484	0.1040	0.0729
E=0.8	Nu_m	Present work	3.5618	3.8156	6.3079	9.9082	16.6032
		Cheikh et al	3.5532	3.8047	6.2942	9.9160	16.7432
		Aminossadati et al	3.5551	3.8060	6.2944	9.9159	16.6779
	T_{max}	Present work	0.3642	0.3634	0.2493	0.1702	0.1162
		Cheikh et al	0.3642	0.3635	0.2494	0.1701	0.1163
		Aminossadati et al	0.3642	0.3635	0.2495	0.1700	0.1160

Finally, for the various Rayleigh number considered. The maximum difference between the mean Nusselt number and the maximum temperature obtained by the present results and the above results are 0.72% and 0.68%, respectively.

Grid Independence Study

In order to select a proper grid density, various grids are employed to simulate the fluid flow and heat transfer within the enclosure at E=0.4, D=0.5 and Ra $= 10^6$. The nanofluid inside enclosure is Cu-water with ∅=0.1. The four different grid sizes are present in Table 3. The Grid size 3 changed grid shape from rectangular to triangular, that decreases the thickness of the boundary layer computation at higher Rayleigh number. Also the Grid size 3 increases grid element in two vertical side-walls, which due to the buoyant flow occur mainly on the two vertical side-walls. Figure 5 shows the result of local Nusselt number along the left heated source surface. The Grid size 3 has smoother curve of local Nusselt number than others especially at two end of the heated source.

Table 3. Different gird sizes for grid independent study

Grid size	grid elements in each horizontal side-wall	grid elements in each vertical side-wall	grid shape	Total grid elements
Grid size 1	20	20	rectangular	400
Grid size 2	40	40	rectangular	1600
Grid size 3	80	100	triangular	19116
Grid size 4	120	120	rectangular	14400

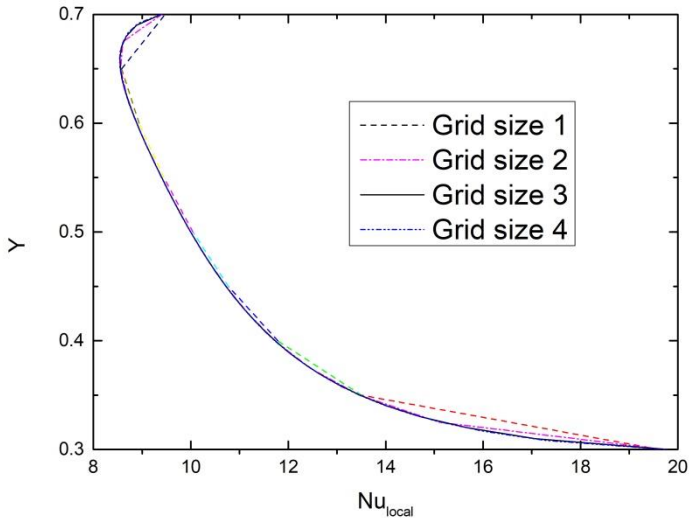

Figure 3. The local Nusselt number along the left heated source for various grid sizes (Cu-water, ∅ $= 0.1$, Ra $= 10^6$, E=0.4, D=0.5)

Table 4 presents the result of the maximum temperature within the enclosure for different Rayleigh numbers and grid sizes. For each Rayleigh number, the value of maximum temperature within enclosure increases from Grid size 1 to Grid size 4, but the value between Grid size 3 and Grid size 4 are almost the same. Finally, the simulations show that the Grid size 3 is sufficiently fine to describe the buoyant flow inside the enclosure.

Table 4. The maximum temperature within enclosure for different Rayleigh numbers and grids (Cu-water, $\emptyset = 0.1$, E=0.4, D=0.5)

Grid size	$Ra = 10^3$	$Ra = 10^4$	$Ra = 10^5$	$Ra = 10^6$	$Ra = 10^7$
Grid size 1	0.37399	0.31321	0.19211	0.11654	0.06976
Grid size 2	0.37441	0.31331	0.19223	0.11688	0.07235
Grid size 3	0.37441	0.31329	0.19247	0.11702	0.07244
Grid size 4	0.37442	0.31331	0.1925	0.1171	0.07255

Results and Discussion

The nanofluid-filled enclosure is studied by three different lengths (E=0.2, E=0.4 and E=0.8) and different types of nanofluids and various volume fractions. The Prandtl number is chosen to be 6.2 for all simulations.

Figure 4 shows the streamlines (on the left) and isotherms (on the right) for Cu-water ($\emptyset$=0.2) nanofluid (plotted by solid line) and pure water (plotted by dashed line) at various Rayleigh numbers when E=0.4 and D=0.5. Since the left and right vertical walls of the enclosure are located heated and cooled sources, which causes buoyant flow along this two side-walls. As the Rayleigh number increases, the buoyant flow strength also increases that causes the boundary layers to become more distinguished. When Rayleigh number equal to 10^6, Cu-water presents an oval shaped rotating cell in the right-center as shown Figure 4(d). For $Ra=10^7$, Figure 4(e) presents the oval shaped rotating cell break up into two small rotating cells, one flows near the right side-wall and another was observed near the left side-wall.

Figure 4(a) and (c) shows the isotherm is distributed gather near the heated source on the left side-wall and tends to be paralleled near the right cooled side-wall. Equation (17) presents $\frac{\partial\theta}{\partial X} = -\frac{k_f}{k_{nf}}$ depends on the ratio of thermal conductivity along the heated source surface (for X=0 and D-0.5E≤Y≤D+0.5E). The value of $\frac{\partial\theta}{\partial X}$ equal to -1 and -0.5897 for pure water and Cu-water nanofluid, which means the tangent angle of isotherm to the X direction along heated source are -45° and -30.528° for pure water and Cu-water nanofluid, respectively. Cu-water's isotherms present shaper than pure water.

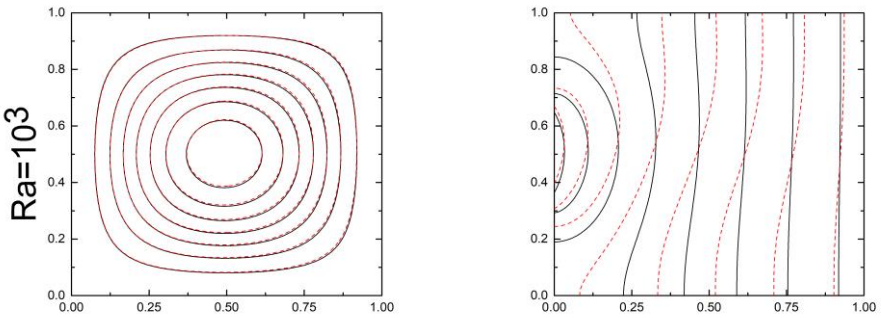

(a)

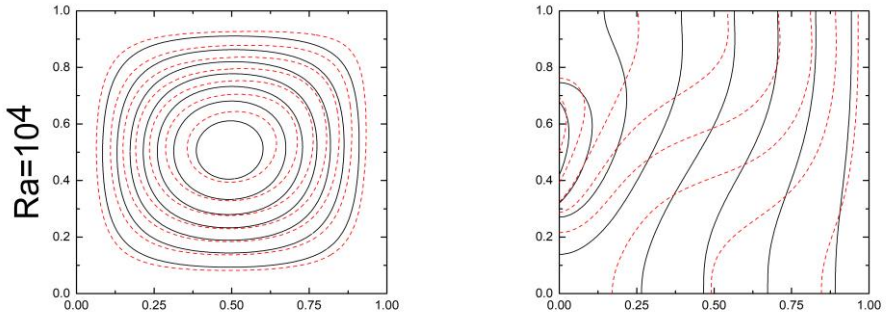

(b)

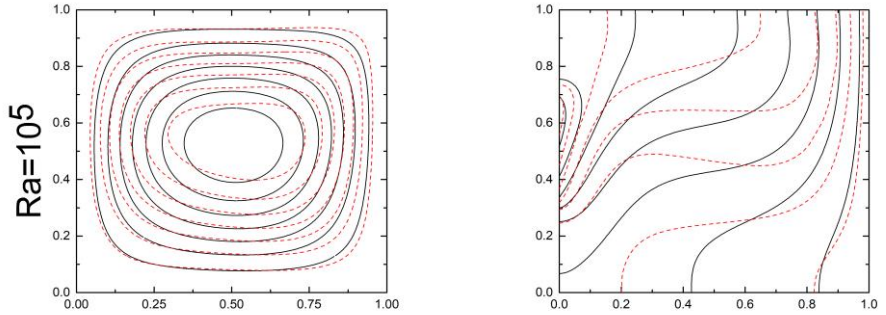

(c)

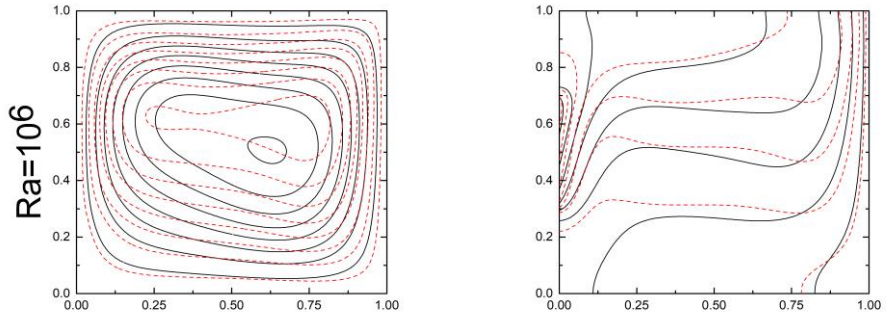

(d)

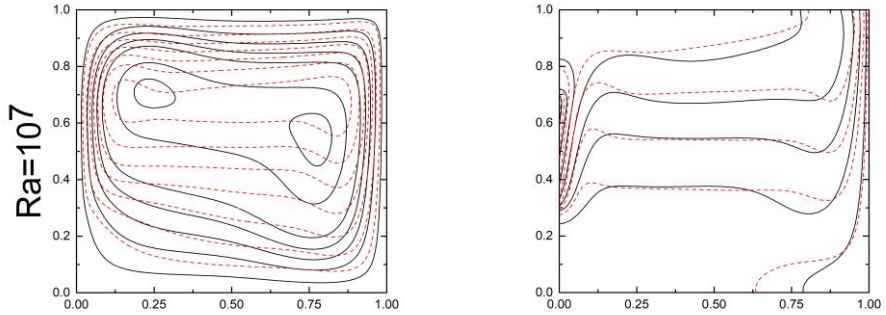

(e)

Figure 4. Streamline (on the left) and isotherm (on the right) of pure water (plotted by dashed line) and Cu-water (Ø=0.2) nanofluid (plotted by solid line) at various Rayleigh numbers (E=0.4, D=0.5, (a)Ra=10^3, (b)Ra=10^4, (c)Ra=10^5, (d)Ra=10^6, (e)Ra=10^7)

The result of local Nusselt number along the heated source for different volume fraction is shown in Figure 5. It is noted that the maximum value of the local Nusselt number is presented as $\emptyset = 0.2$ and the minimum value as shown for $\emptyset = 0$. As the increasing volume fraction, the value of the local Nusselt number also increases that due to the enhancement of convection within the enclosure.

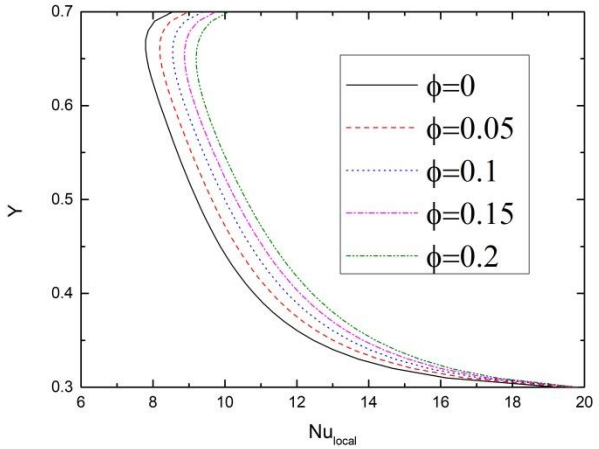

Figure 5. The local Nusselt number on the heated source for various volume fraction (Cu-water, Ra=10^6, D=0.5, E=0.4)

Figure 6 presents the result of the maximum surface temperature on the heated source for various volume fraction and Rayleigh number. The surface temperature on heated source is not uniform and the maximum value is reduced by increasing volume fraction for all range Rayleigh number. The maximum temperature decreases much more rapidly for a higher volume fraction. This reduction is due to the higher volume fraction improves the thermal conductivity of the nanofluid and shifts the heat transfer from conduction to convection inside the enclosure.

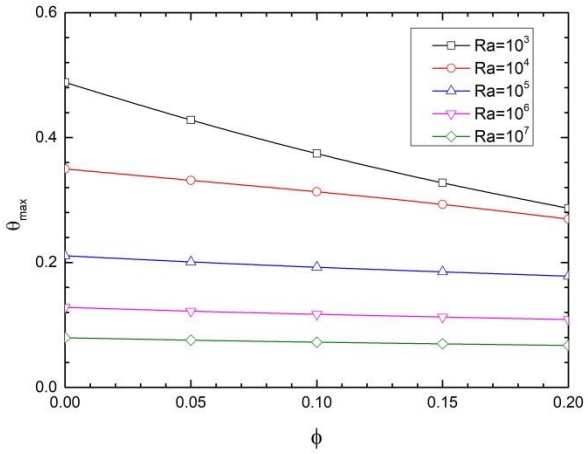

Figure 6. The maximum temperature on the heated source for various volume fraction and Rayleigh number (Cu-water, D=0.5, E=0.4)

Figure 7 exhibits the streamlines (on the left) and isotherms (on the right) of Cu-water (Ø=0.1) nanofluid at various heated source's length. The comparison between 0.8E heated source length (plotted by solid line) and 0.2E heated source length (plotted by dashed line) are presented that counter rotating cells are formed in clockwise direction for both situations. As the increasing heated source length, the cell boundaries become more distinguished on side-walls, which mean the buoyant flow strength increases in the enclosure. Isotherms show that temperature gradients near 0.8E heated source become more sever along both vertical side-walls that can be explained as the higher heat transport rate is generated by increasing heated source.

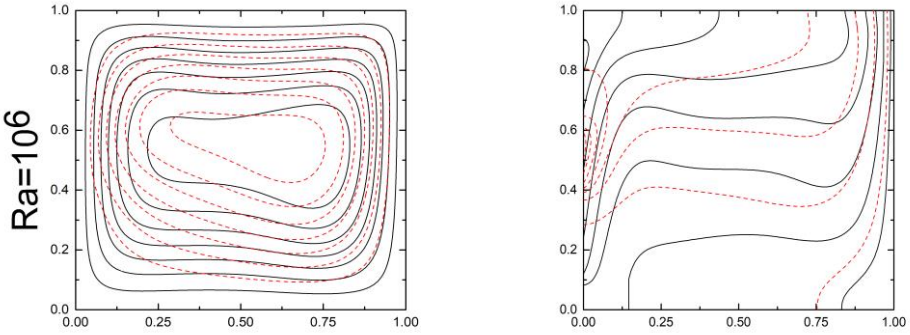

Figure 7. Streamlines (on the left) and isotherms (on the right) of Cu-water (Ø=0.1) nanofluid for different heated source length, E=0.2 (plotted by dashed line) and E=0.8 (plotted by solid line) (D=0.5, Ra=10^6)

Figure 8 shows the results of the maximum temperature at heated source for different heated source lengths. As increases the heated source's length, the maximum temperature also increases for all range Rayleigh number. It is due to the longer heated source length causes higher heat flux transfer. But the maximum temperature decreases as Rayleigh number increases that can be explained as more heat flux away from heated source surface by stronger flow strength.

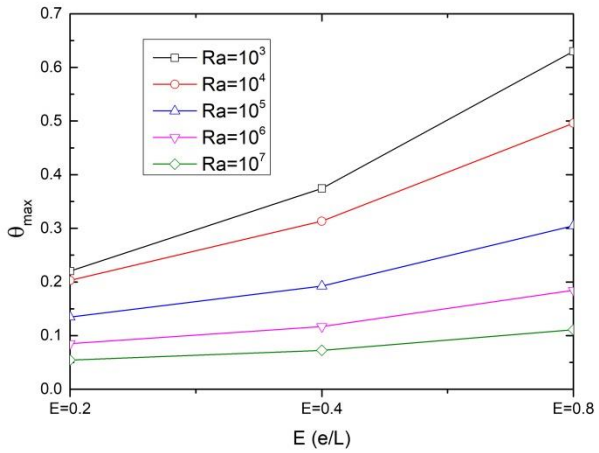

Figure 8. The maximum temperature on the heated source for various heated source lengths and Rayleigh number (Cu-water nanofluid, Ø=0.1, D=0.5)

In order to study the fluid flow inside the enclosure, Figure 9 presents the result of U-velocity (component velocity in x-direction) in mid-section centerline of enclosure (from (0.5, 0) to (0.5, 1)) for various heated source lengths. The strength of fluid flow enhances near two vertical side-walls and descends in the center of the enclosure, which due to stronger buoyant flow near the two side-walls. The U-velocity increases by increasing the length of heated source because of higher heat generation rates between left and right side-walls.

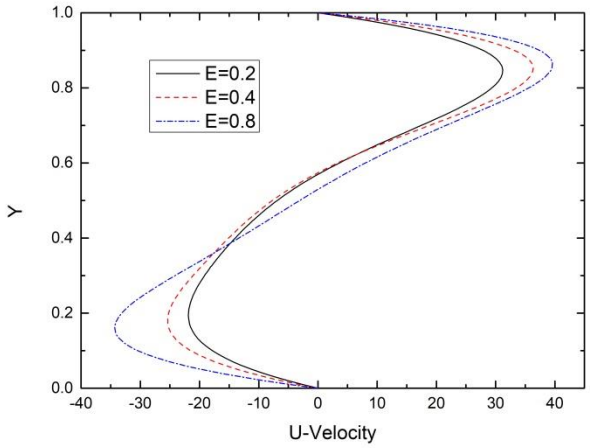

Figure 9. U-velocity at mid-section V (0.5, Y) of the enclosure for various heated source lengths (Cu-water, Ø=0.1, D=0.5, Ra=10^6)

Figure 10 presents the result of local Nusselt number along the heated source for different types of nanofluids. Cu has the highest local Nusselt number value and the lowest value is pure water. Compared between three different nanofluids, TiO_2 has the lowest local Nusselt number because it has the lowest value of thermal conductivity as shown in Table 1. On the other hand, Cu has the highest value of thermal conductivity that indicates the local Nusselt number increases by increasing thermal conductivity.

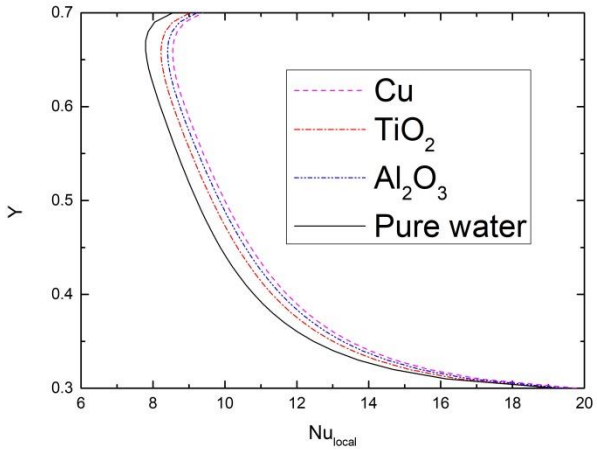

Figure 10. The local Nusselt number on the heated source for various types of nanofluids (D=0.5, E=0.4, Ra=10^6, Ø=0.1)

The result of mean Nusselt number on the heated source for different types of nanofluids are shown in Figure 11. The mean Nusselt number increases with increasing volume fractions and the lowest value of mean Nusselt number was generated by TiO_2 for all range Rayleigh number as the same situation as the local Nusselt number results. That also due to TiO_2 has lowest thermal conductivity value compared with the other nanoparticles. Figure 11(f) exhibits the different of mean Nusselt number become larger as increasing Rayleigh number that due to high Rayleigh number causes stronger heat transfer within the enclosure. Moreover, the value of thermal conductivity of Al_2O_3 is approximately one tenth of Cu (Table 1), but Al_2O_3 has low thermal diffusivity that causes the mean Nusselt number of Al_2O_3 is lower than that for Cu at high Rayleigh number but almost the same at low Rayleigh number.

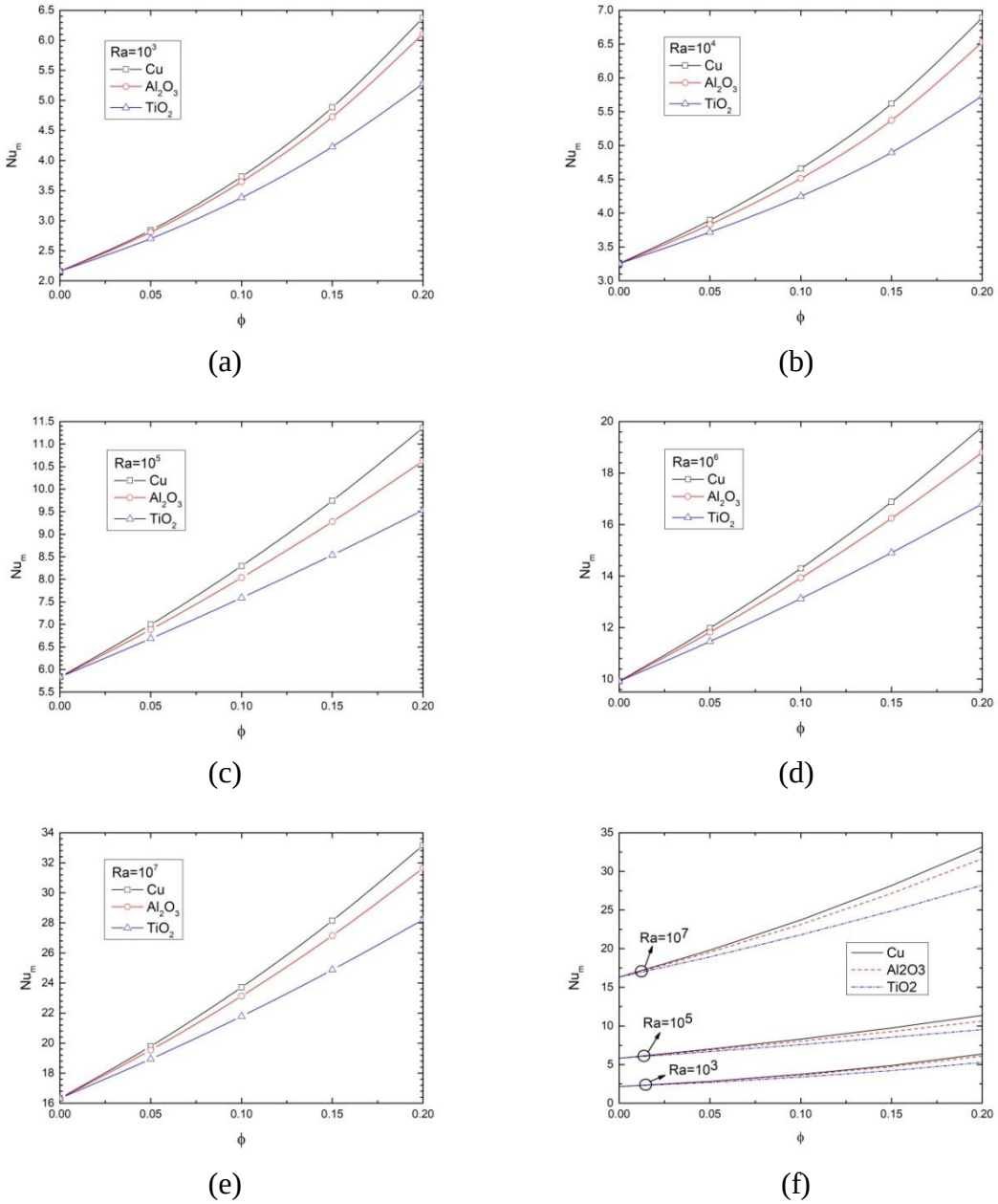

Figure 11. The mean Nusselt number on the heated source for different types of nanofluids as various volume fractions and Rayleigh number (D=0.5, E=0.4, (a)Ra=10^3, (b)Ra=10^4, (c)Ra=10^5, (d)Ra=10^6, (e)Ra=10^7, (f)Ra=10^3, 10^5 *and* 10^7)

Figure 12 shows result of V-velocity at mid-section centerline of the enclosure (from (0, 0.5) to (1, 0.5)) for various types of nanofluids. The V-velocity indicated a parabolic variation near two vertical side-walls and almost zero at X from 0.4 to 0.6 that means the fluid flow almost stopped in the center of the enclosure. The V-velocity of nanofluids is lower than the pure water that can be explained as nanoparticle's suspension affects the buoyant flow. To clarify the effects of nanofluid on reduction of temperature along heated source surface, Table 4 displays the maximum temperature on the heated source for various nanofluids as different volume fractions. Compared with the pure water, nanofluids provide temperature reduction on the heated source surface and Cu has the best cooling performance.

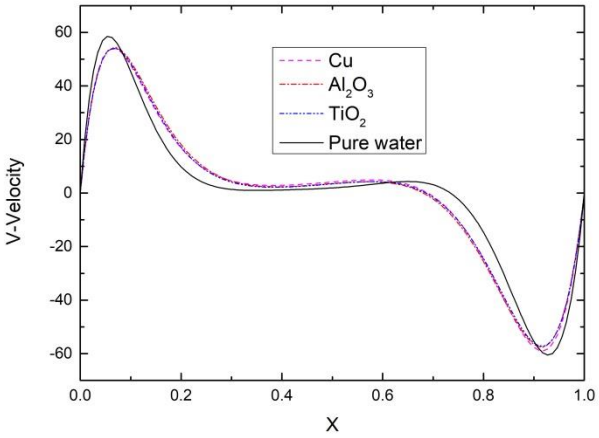

Figure 12. V-velocity at mid-section V(X, 0.5) of the enclosure for different types of nanofluids (D=0.5, E=0.4, Ra=10^6 and Ø=0.1)

Table 4. The maximum temperature on heated source (E=0.4, D=0.5) for pure water and different types of nanofluids at various Rayleigh number and volume fraction

		Rayleigh Number				
		Ra=10^3	Ra=10^4	Ra=10^5	Ra=10^6	Ra=10^7
	Pure water	0.488	0.350	0.211	0.128	0.080
Ø=0.05	Cu	0.428	0.332	0.201	0.122	0.076
	Al_2O_3	0.431	0.335	0.203	0.123	0.076
	TiO_2	0.439	0.339	0.205	0.125	0.077
Ø=0.1	Cu	0.374	0.313	0.192	0.117	0.072
	Al_2O_3	0.379	0.319	0.196	0.119	0.073
	TiO_2	0.393	0.327	0.201	0.122	0.075
Ø=0.15	Cu	0.328	0.293	0.185	0.113	0.070
	Al_2O_3	0.333	0.301	0.191	0.115	0.071
	TiO_2	0.352	0.313	0.197	0.119	0.073
Ø=0.2	Cu	0.287	0.270	0.178	0.109	0.067
	Al_2O_3	0.293	0.278	0.186	0.113	0.069
	TiO_2	0.315	0.295	0.194	0.117	0.072

Conclusions

Natural convection in a nanofluid-filled enclosure with partially heated source on the left side-wall has been numerically simulated. The effect of heat transfer and fluid flow within the enclosure by various volume fractions, various heated source lengths and different types of nanofluids were investigated. The results show as

- The increase of Rayleigh number causes increasing mean Nusselt number on heated source and enhances the fluid flow and temperature gradient on the two vertical side-walls.
- Increasing the length of heated source enhances heat generation rates, which causes both the maximum temperature on the heated source surface and flow strength within the enclosure increased.
- The increase of volume fractions improves the thermal conductivity of the nanofluid and shifts more heat flux from conduction to convection, that observed by the increasing local Nusselt number and maximum temperature on the heated source.
- Nanofluids (Cu, Al_2O_3 and TiO_2) reduce the fluid flow strength inside the enclosure and the maximum temperature on heated source surface. The best cooling performance by using Cu-water because it has the highest value of thermal conductivity among the three nanofluids.

Reference

[1] Eastman J.A., Phillpot S.R., Choi S.U.S., Keblinski P.. (2004) THERMAL TRANSPORT IN NANOFLUIDS, *Annual Review of Materials Research, Vol.34*, 219–246.

[2] Das S.K., Choi S.U.S., Patel H.E.. (2006) Heat Transfer in Nanofluids-A Review, *Journal Heat Transfer Engineering, volume27,2006-Issue 10 Journal*, 3–19.

[3] Kleinstreuer C. and Feng Y.. (2011) Experimental and theoretical studies of nanofluid thermal conductivity enhancement: a review, *A SpringgerOpen Journal*, 1–13.

[4] Keblinski P., Eastman J.A., Cahill D.G.. (2005) Nanofluid for thermal transport, *Materialstoday,Volume8, Issue6*, 36–44.

[5] Masuda H., Ebata A., Teramea K. and Hishinuma N.. (1993) Alteration of thermal conductivity and viscosity of liquid by dispersing ultra-fine particles, *Netsu Bussei 1993,4*, 227-223.

[6] Eastman J.A., Choi U.S., Li S., Thompson L.J., Lee S.. (1997) Enhanced thermal conductivity through the development of nanofluid, *In Nanophase and Nanocomposite Materials II*, 3-11.

[7] Oztop H.F. and Abu-Nada E.. (2008) Numerical study of natural convection in partially heated rectangular enclosures filled with nanofluid, *International Journal of Heat and Fluid Flow 29 (2008)*, 1326-1336.

[8] Sheikhzadeh G.A., Arefmanesh A., Kheirkhah M.H., Abdollahi R.. (2010) Natural convection of Cu-water nanofluid in a cavity with partially active side walls, *European Journal of Mechanics B/Fluids 30 (2011)*, 166-176.

[9] Cheikh N.B., Beya B.B., Lili T.. (2007) Influence of thermal boundary conditions on natural convection in a square enclosure partially heated from below, *International Communications in Heat and Mass Transfer 34 (2007)*, 369-379.

[10] Amoinossadati S.M. and Ghasemi B.. (2009) Natural convection cooling of a localized heat source at the bottom of a nanofluid-filled enclosure, *European Journal of Mechanics B/Fluid 28 (2009)*, 630-640.

[11] Abu-Nada E., Masoud Z., Hijazi A.. (2008) Natural convection heat transfer enhancement in horizontal concertric annuli using nanofluids, *Int. Comm. Heat mass Transfer 35 (5) (2008)*, 657-665.

[12] Brinkman H.C.. (1952) The viscosity of concentrated suspensions and solution, *H. Chem. Phys. 20*, 571-581.

[13] Maxwell J. (1904) A Treatise on Electricity and Magnetism, *Second ed. Oxford University Press, Cambridge,UK*.